Depalmitoylated Ras traffics to and from the Golgi complex via a nonvesicular pathway

J. Shawn Goodwin,[1] Kimberly R. Drake,[1] Carl Rogers,[1] Latasha Wright,[3] Jennifer Lippincott-Schwartz,[2] Mark R. Philips,[3] and Anne K. Kenworthy[1,2]

[1]Department of Molecular Physiology and Biophysics and Department of Cell and Developmental Biology, Vanderbilt University School of Medicine, Nashville, TN 37232
[2]Cell Biology and Metabolism Branch, National Institute of Child Health and Human Development, National Institutes of Health, Bethesda, MD 21218
[3]Department of Cell Biology, New York University School of Medicine, New York, NY 10016

Palmitoylation is postulated to regulate Ras signaling by modulating its intracellular trafficking and membrane microenvironment. The mechanisms by which palmitoylation contributes to these events are poorly understood. Here, we show that dynamic turnover of palmitate regulates the intracellular trafficking of HRas and NRas to and from the Golgi complex by shifting the protein between vesicular and nonvesicular modes of transport. A combination of time-lapse microscopy and photobleaching techniques reveal that in the absence of palmitoylation, GFP-tagged HRas and NRas undergo rapid exchange between the cytosol and ER/Golgi membranes, and that wild-type GFP-HRas and GFP-NRas are recycled to the Golgi complex by a nonvesicular mechanism. Our findings support a model where palmitoylation kinetically traps Ras on membranes, enabling the protein to undergo vesicular transport. We propose that a cycle of depalmitoylation and repalmitoylation regulates the time course and sites of Ras signaling by allowing the protein to be released from the cell surface and rapidly redistributed to intracellular membranes.

Introduction

The small GTPase Ras is a major regulator of cell growth, death, and differentiation (Katz and McCormick, 1997; Olson and Marais, 2000; Shields et al., 2000; Downward, 2003). Ras is targeted to the inner leaflet of the plasma membrane by two motifs contained in its COOH-terminal hypervariable domain. The first, shared by all the ubiquitously expressed Ras isoforms (H-, N-, and KRas), is a COOH-terminal CAAX motif that undergoes posttranslational modification by sequential farnesylation, proteolysis, and carboxyl methylation (Clarke, 1992). The second varies between Ras isoforms, consisting of a polybasic domain for KRas 4B and either one or two palmitoylation sites for NRas, HRas, and KRas 4A (Hancock et al., 1989, 1990, 1991a,b). Palmitoylation involves the reversible posttranslational modification of cysteine residues by the addition of a palmitate through a thioester linkage (Smotrys and Linder, 2004). Farnesylation is absolutely required for binding of Ras to cell membranes and Ras signaling, while mutations of the "second signal" (i.e., the polybasic domain or palmitoylation sites) partially disrupt membrane binding and lead to aberrant signaling (Willumsen et al., 1984; Hancock et al., 1990; Kato et al., 1992; Chiu et al., 2002).

The hypervariable domain additionally functions to regulate the subcellular distribution, intracellular trafficking, and membrane microenvironment of Ras. The CAAX motif targets Ras to the cytosolic face of the ER and Golgi apparatus, and exit of Ras from these compartments requires either palmitoylation or the polybasic domain (Choy et al., 1999; Apolloni et al., 2000). How trafficking of Ras to the cell surface is accomplished depends on the nature of the second signal. The palmitoylated Ras isoforms HRas and NRas are delivered from the Golgi complex to the cell surface as part of the secretory pathway, whereas KRas 4B reaches the plasma membrane by an unknown mechanism that is independent of vesicular transport. The COOH-terminal membrane targeting motifs of Ras appear to contain the relevant signals for Ras trafficking, as these motifs traffic GFP to the plasma membrane in a similar manner as the full-length protein (Choy et al., 1999; Apolloni et al., 2000). In adipocytes and yeast, HRas can traffic to the plasma membrane by a nonclassical secretory transport pathway as well as the classic secretory pathway (Dong et al., 2003; Watson et al., 2003). Palmitoylated forms of Ras are also often found associated with the Golgi complex where they can signal,

Correspondence to Anne Kenworthy: anne.kenworthy@vanderbilt.edu

Abbreviations used in this paper: 2BP, 2-bromo-palmitate; CTXB, cholera toxin B subunit; FCS, fluorescence correlation spectroscopy; Mf, mobile fraction; τ_D, correlation time; PAT, palmitoyl acyl transferase.

The online version of this article includes supplemental material.

The Journal of Cell Biology, Vol. 170, No. 2, July 18, 2005 261–272
http://www.jcb.org/cgi/doi/10.1083/jcb.200502063

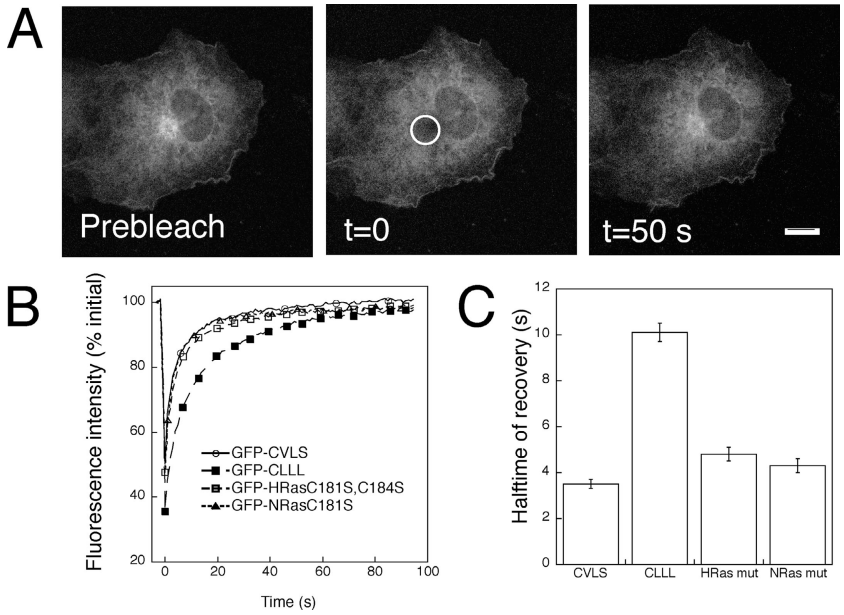

Figure 1. **GFP-CAAX proteins and GFP-Ras palmitoylation mutants traffic rapidly between the ER and Golgi complex.** (A) The Golgi-associated pool of a GFP-HRas C181S, C184S recovers rapidly and completely within 1 min after photobleaching of the entire Golgi complex (circle, t = 0). Bar, 10 μm. (B) Kinetics of fluorescence recovery after bleaching the entire Golgi-associated pool of GFP-CVLS (circles), GFP-CLLL (closed squares), GFP-HRas C181S, C184S (open squares), and GFP-NRas C181S (triangles). Data are from a representative experiment. For clarity, error bars are not shown. (C) Halftimes of fluorescence recovery for Golgi photobleaching experiments. Data are the mean ± SE from four independent experiments (~10 cells per experiment). Golgi bleaches were performed at 22°C.

providing a mechanism for regulation of isoform-specific Ras signaling via their distinct subcellular localizations (for review see Bivona and Philips, 2003; Hancock, 2003). The hypervariable domain further contributes to specificity of Ras signaling through different isoforms by targeting the proteins to spatially and compositionally distinct plasma membrane microdomains (for review see Hancock, 2003; Parton and Hancock, 2004).

How palmitoylation contributes to the isoform-specific trafficking and signaling of Ras has not been fully established. One proposed function of palmitoylation is to enhance Ras binding to membranes (Silvius and l'Heureux, 1994; Shahinian and Silvius, 1995; Silvius, 2002). Palmitoylation may also regulate the sorting of Ras into vesicles destined for the cell surface or targeted for clathrin-independent endocytosis (Smotrys and Linder, 2004). Both mechanisms could be potentially modulated in a dynamic manner, as the palmitates on NRas and HRas undergo dynamic turnover within minutes to hours (Magee et al., 1987; Lu and Hofmann, 1995; Baker et al., 2000, 2003). How this turnover is regulated and its significance for Ras biology is not yet known, as the enzymes involved in the regulation of Ras palmitoylation and depalmitoylation have only recently begun to be identified (Linder and Deschenes, 2003, 2004; Dietrich and Ungermann, 2004; Smotrys and Linder, 2004).

In this study, we examined the role of palmitoylation in the intracellular transport of HRas and NRas to and from the Golgi complex. Using quantitative fluorescence microscopy and photobleaching techniques, we show that GFP-tagged mutants of HRas and NRas lacking functional palmitoylation sites undergo rapidly reversible binding to the ER and Golgi complex. We also provide evidence that wild-type NRas and HRas undergo a cycle of depalmitoylation and repalmitoylation that allows them to recycle to the Golgi complex. We propose that the reversible palmitoylation of Ras allows the protein to shift between vesicular and nonvesicular modes of transport, and ultimately controls the location and time course of intracellular Ras signaling.

Results

GFP-CAAX and GFP-Ras palmitoylation mutants traffic extremely rapidly to the Golgi complex

Two models could explain why NRas and HRas are retained in the ER and Golgi complex in the absence of palmitoylation (Choy et al., 1999; Apolloni et al., 2000). First, Ras could undergo vesicular transport between the ER and Golgi complex, but require palmitoylation to allow it to enter into Golgi-derived vesicles destined for the cell surface (Choy et al., 1999). Second, the membrane binding affinity of the protein could be reduced in absence of palmitoylation, allowing it to undergo reversible binding to ER and Golgi membranes (Hancock et al., 1989, 1991b; Shahinian and Silvius, 1995). To distinguish between these possibilities, we used photobleaching techniques to study the kinetics of transport of GFP-tagged NRas and HRas palmitoylation mutants to the Golgi complex in COS-7 cells. For comparison, we also examined GFP-CVLS, a substrate for farnesylation, and GFP-CLLL, a substrate for geranylgeranylation (Choy et al., 1999). After photobleaching the fluorescent proteins localized to the Golgi complex, recovery of fluorescence from outside the bleach region occurred extremely rapidly and completely, with a half time of <10 s and a mobile fraction (Mf) of $>95\%$ (Fig. 1). Recovery kinetics were identical for the GFP-HRas and GFP-NRas palmitoylation mutants, whereas the recovery of GFP-CLLL was twofold slower (Fig. 1 C). These rapid rates of recovery are several orders of magnitude faster than the kinetics of typical vesicular transport from the ER to the Golgi for the transmembrane proteins VSVG-GFP and GalTase-GFP (rate constants of 2.8%/min and 3.6%/min, respectively) (Hirschberg et al., 1998; Zaal et al., 1999), but are consistent with a rapidly reversible membrane binding event.

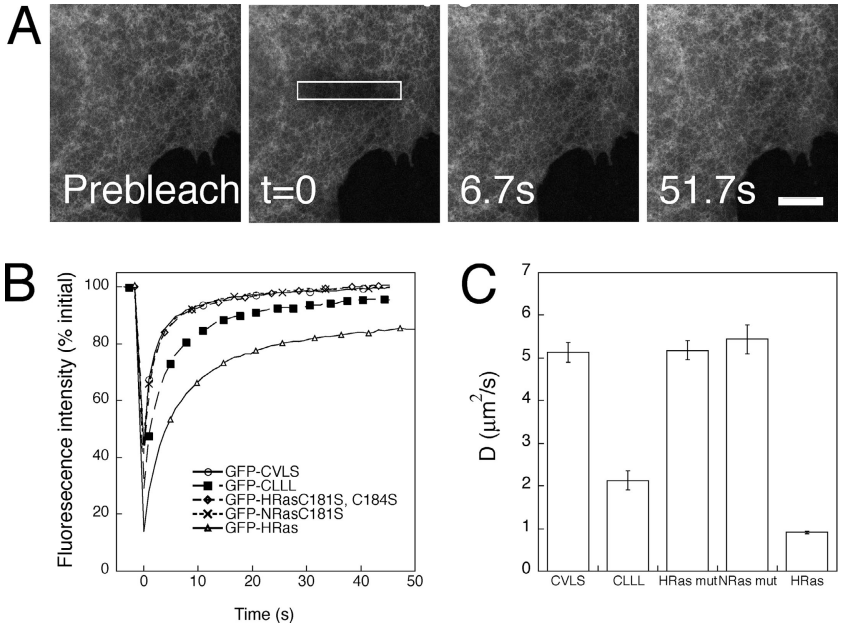

Figure 2. **Diffusional mobilities of GFP-CAAX proteins and GFP-Ras palmitoylation mutants in the ER measured by confocal FRAP.** (A) Representative images from a confocal FRAP measurement of the lateral diffusion of GFP-NRasC181S in the ER. The bleach box (white) is 4 μm deep. Recovery occurs so rapidly that it is difficult to see the bleached region at the 6.7-s time point. Bar, 10 μm. (B) Recovery curves from ER-associated pools of GFP-CVLS (circles), GFP-CLLL (squares), GFP-HRas C181S, C184S (diamonds), and GFP-NRas C181S (crosses); t = 22°C. Data are from a representative experiment (n = 10 cells/protein; mean ± SE). For comparison, a recovery curve for GFP-HRas at the cell surface is shown (triangles). (C) D for ER-associated protein calculated from confocal FRAP experiments. D for GFP-HRas at the cell surface is shown for comparison.

Diffusional mobility measurements confirm that a fraction of CAAX-containing proteins are present as a soluble pool

We next asked whether the ER-associated pools of protein likewise underwent reversible exchange with a soluble pool. To test this, FRAP measurements were performed using a 4-μm-wide strip centered on the ER while monitoring the fluorescence in the surrounding region of the cell (Fig. 2 A). Identical recovery curves were obtained for the two Ras palmitoylation mutants and GFP-CVLS, whereas the recovery of GFP-CLLL was slightly slowed (Fig. 2 B). Mf for all proteins examined was >90%. The apparent diffusion coefficients (D) were ~5 $\mu m^2/s$ for the palmitoylation mutants and GFP-CVLS (Fig. 2 C), a value 10-fold faster than the diffusion coefficient for the transmembrane protein VSVG-GFP in the ER (Nehls et al., 2000). D for GFP-CLLL was significantly slower, ~2 $\mu m^2/s$, but was still twofold faster than the diffusional mobility of GFP-HRas on the cell surface under identical conditions (Fig. 2, B and C) (see also Niv et al., 2002; Kenworthy et al., 2004). These recoveries are too fast to occur as the result of lateral diffusion within the ER membrane, but could be explained if the recovery was the result of a combination of membrane exchange and lateral diffusion of both membrane-bound and cytosolic pools of the protein (Rotblat et al., 2004).

To test this idea further we used a second technique to measure protein diffusional mobility—fluorescence correlation spectroscopy (FCS; for review see Dittrich et al., 2001). Importantly, FCS can resolve two or more diffusing species, and is also more sensitive to the diffusion of soluble proteins than our confocal FRAP assay due to its higher temporal resolution. Although the autocorrelation curve for cytoplasmic GFP was well described by a one-component fit with a characteristic D of ~45 $\mu m^2/s$, autocorrelation curves for the Ras palmitoylation mutants and GFP-CAAX proteins in the ER region were shifted to a longer correlation time (τ_D) (indicative of a slower D), and required a two-component fit to describe the data (Fig. 3, A and B). D for the faster component (D_1) was

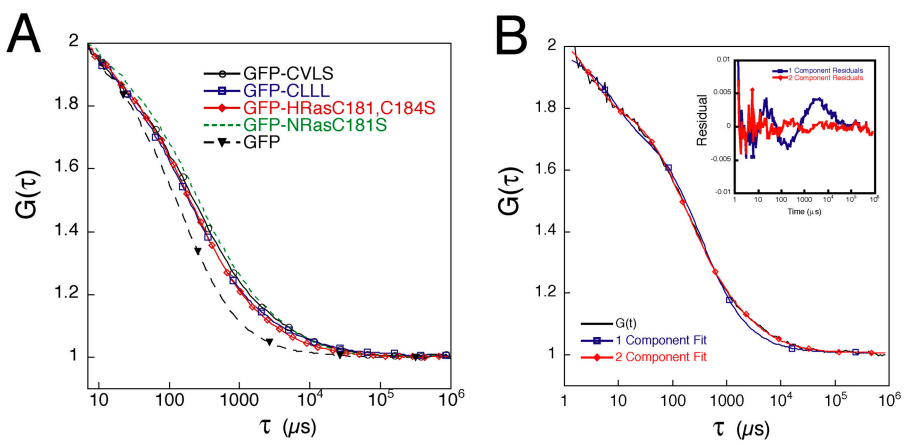

Figure 3. **FCS detects both a soluble and membrane-associated pool of GFP-CAAX proteins and GFP-Ras palmitoylation mutants.** (A) Normalized FCS autocorrelation curves for GFP-CVLS (circles), GFP-CLLL (squares), GFP-HRas C181S, C184S (diamonds), and GFP-NRasC181S (dotted line) measured in the ER. As a control, measurements were also made for cytosolic GFP (inverted triangle) under similar conditions. Each curve is the average of 10 measurements on an individual cell from a representative experiment. (B) A two-component model (red) rather than a one-component model (blue) is required to describe the autocorrelation data for GFP-CVLS. The τ_D for the fast component (174 μs) is similar to free GFP, whereas τ_D for the slower component (3,195 μs) corresponds to D of 2.3 $\mu m^2/s$. The inset shows a plot of the residuals for each fit. FCS data were obtained at 22°C.

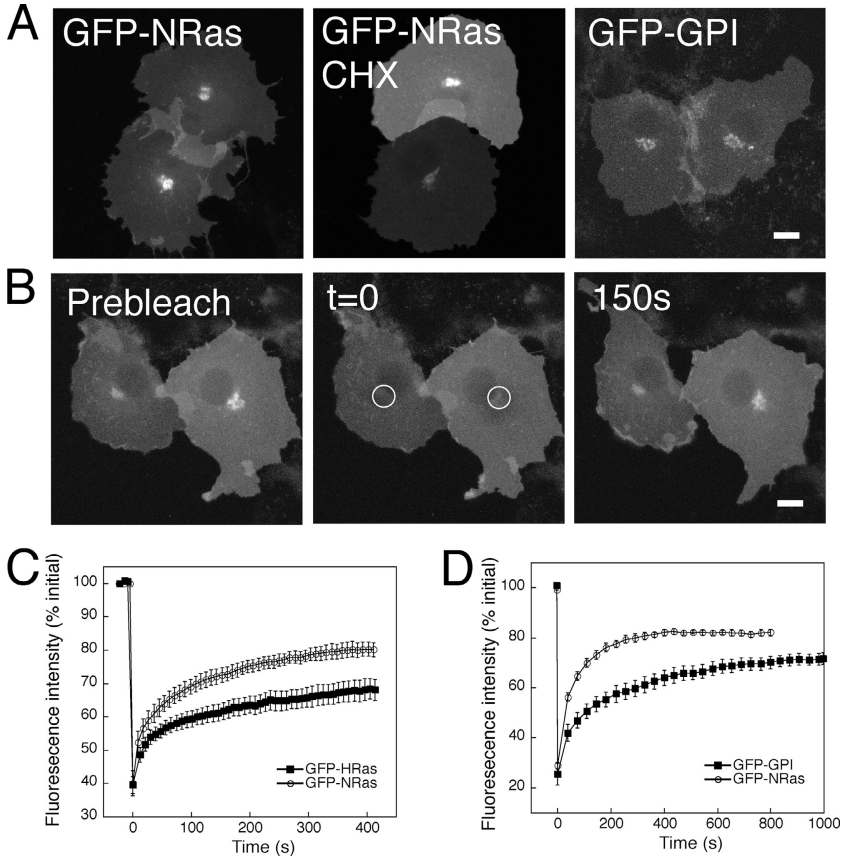

Figure 4. **GFP-NRas and GFP-HRas are trafficked to the Golgi complex in the absence of new protein synthesis under steady-state conditions.** (A) GFP-NRas is localized to the Golgi complex in the absence of new protein synthesis. Cells were either mock treated (control) or incubated in the presence of 200 μg/ml cycloheximide (CHX) for 4 h at 37°C before imaging. For comparison, the distribution of GFP-GPI, a protein that cycles between the Golgi complex and cell surface, is shown. Bar, 10 μm. (B) The Golgi-associated pool of GFP-NRas partially recovers after photobleaching of the entire Golgi compartment (white circles, t = 0). Cells were treated with cycloheximide for 4 h before the experiment. Bar, 10 μm. (C) Kinetics of recovery of fluorescence in the Golgi complex for GFP-HRas (closed squares) and GFP-NRas (open circles) at 37°C (n = 8–9 cells). Note the differences in the extent of recovery for the two proteins. Data are from a representative experiment. Similar results were obtained in the presence or absence of cycloheximide. Bars = SE. (D) Kinetics of Golgi recovery for GFP-NRas (open circles) versus GFP-GPI (closed squares) at 37°C (n = 6–9 cells). Bars = SE.

similar to that of GFP alone, whereas D for the slower component (D_2) was identical within error (~2.6 $\mu m^2/s$) for all the proteins except GFP-CLLL (Table I). These findings support the notion that two pools of protein, one soluble and one reversibly bound to membranes, exist under the conditions of these experiments.

Two populations of GFP-HRas and GFP-NRas are localized to the Golgi complex under steady-state conditions

We next considered the role of palmitoylation in trafficking wild-type HRas and NRas to the cell surface. Ras is found in the Golgi complex, where it undergoes vesicular transport to the cell surface in BHK and COS cells (Choy et al., 1999; Apolloni et al., 2000). The presence of Ras on the Golgi complex is in part due to the flux of newly synthesized protein through the secretory pathway, as treatment of cells with cycloheximide caused a partial loss of fluorescence from the Golgi complex as assessed by fluorescence microscopy (Choy et al., 1999). However, the Golgi-associated pool of Ras was not completely chased out of the Golgi in pulse–chase experiments (Choy et al., 1999), raising the possibility that one or more pathways may recycle Ras to the Golgi complex in a post-biosynthetic manner.

To test this hypothesis, we first confirmed that GFP-NRas (Fig. 4 A) and GFP-HRas (unpublished data) remain Golgi associated after cycloheximide treatment. We next asked whether Golgi-associated Ras was actively trafficked to the Golgi complex in the absence of new protein synthesis by photobleaching the entire Golgi-associated pool of protein, then monitoring recovery of fluorescence in the area over time (Fig. 4 B). Both GFP-NRas and GFP-HRas recovered after photobleaching, with similar half times (48 ± 9 s vs. 36 ± 5 s, respectively) but to differing extents (64 ± 4% vs. 39 ± 3%, n = 33 and 23 cells, respectively). Thus, a fraction of both wild-type GFP-HRas and GFP-NRas appear to be actively and rapidly recycled to the Golgi complex; the remainder of the protein, which does not recover after the bleach, appears to represent a stably bound pool.

Table I. **Diffusional mobility of GFP-CAAX proteins and GFP-Ras palmitoylation mutants in the ER measured by FCS**

Protein	D_{fast}	% fast component	D_{slow}
	$\mu m^2/s$	%	$\mu m^2/s$
GFP-HRas mutant	43.6 ± 3.4 (13)	79.9 ± 3.0	2.78 ± 0.44
GFP-NRas mutant	47.6 ± 4.2 (16)	75.5 ± 2.6	2.90 ± 0.40
GFP-CVLS	41.9 ± 4.2 (12)	79.4 ± 3.0	2.49 ± 0.72
GFP-CLLL	45.0 ± 3.0 (11)	86.1 ± 1.8	1.18 ± 0.30[a]
GFP	48.8 ± 2.3 (9)	100	-

[a]$P < 0.0001$.

The rapidly recovering population of Golgi-associated GFP-HRas and GFP-NRas is recycled to the Golgi complex by a nonvesicular mechanism

We hypothesized that the rapidly recovering pool of GFP-HRas and GFP-NRas to the Golgi could be delivered there by

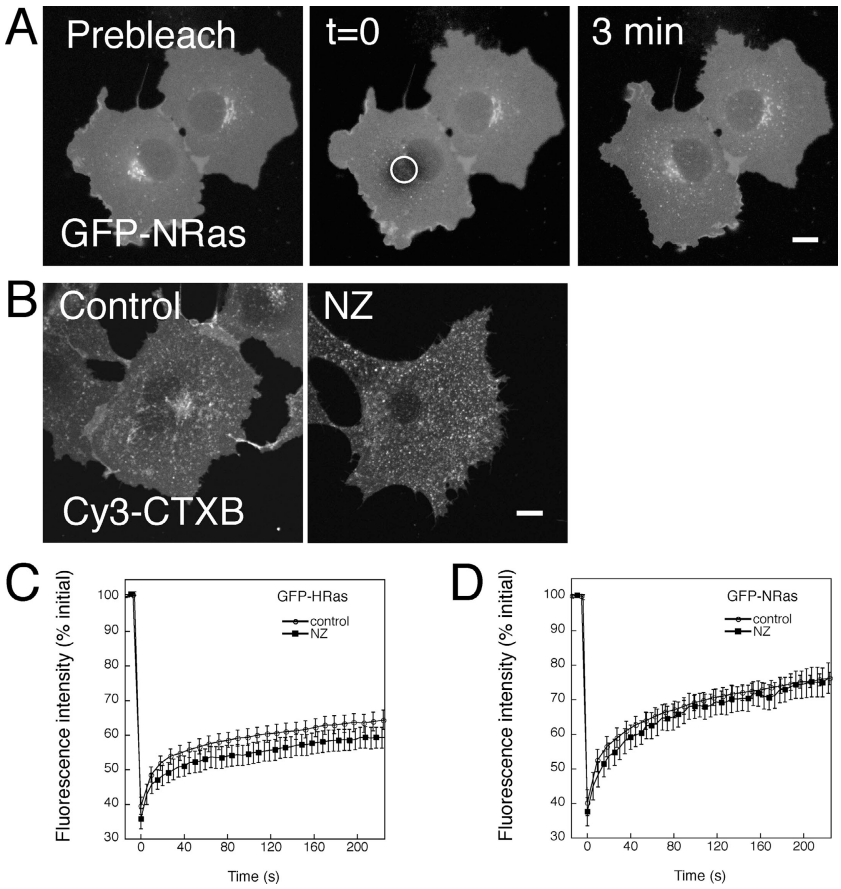

Figure 5. **Recycling of GFP-HRas and GFP-NRas to the Golgi complex occurs by a microtubule-independent pathway.** (A) Cells expressing GFP-NRas were subjected to acute nocodazole treatment as described in the Materials and methods before imaging. The Golgi-associated pool of GFP-NRas was then selectively photobleached (circle, t = 0) and fluorescence recovery was monitored over time. Bar, 10 μm. (B) Acute nocodazole treatment (NZ) inhibits delivery of Cy3-CTXB to the perinuclear region after 20 min of internalization, a time point at which significant Cy3-CTXB accumulation is observed in the perinuclear region in cells treated with vehicle alone (control). Bar, 10 μm. (C and D) Kinetics of recovery of GFP-HRas (C) and GFP-NRas (D) to the Golgi complex are not significantly altered by acute nocodazole treatment. Data are from a representative experiment at 37°C. Bars = SE.

either endocytosis or nonvesicular transport. One candidate endocytic mechanism is a clathrin-independent endocytic pathway used for the internalization of lipid raft–associated proteins and lipids such as GFP-GPI and cholera toxin B subunit (CTXB) from the cell surface to the Golgi complex (Nichols et al., 2001). We therefore compared the recovery of GFP-NRas to GFP-GPI after bleaching of the Golgi region in cycloheximide-treated cells (Fig. 4 D). Golgi refilling of GFP-NRas was significantly more rapid than that of GFP-GPI ($t_{1/2}$ of 7 min) (Nichols et al., 2001), suggesting Ras recovery may occur by an alterative mechanism. To test this possibility further, we examined the effect of microtubule disruption by nocodazole, which inhibits molecules internalized by clathrin-independent pathways from reaching the Golgi complex (Choudhury et al., 2002). In cells subjected to acute nocodazole treatment (Ward et al., 2001), uptake of CTXB to the perinuclear region was inhibited. This treatment had no effect on trafficking of GFP-HRas and GFP-NRas to the Golgi complex, however, suggesting this event does not require vesicular transport (Fig. 5).

Dynamic depalmitoylation of HRas and NRas causes the proteins to redistribute to the ER and Golgi complex

Because Ras palmitoylation mutants are reversibly bound to Golgi membranes (Fig. 1), we considered the possibility that removal of palmitate on Ras could allow the protein to recycle to the Golgi complex by a nonvesicular mechanism. To study the contribution of depalmitoylation to Ras localization and

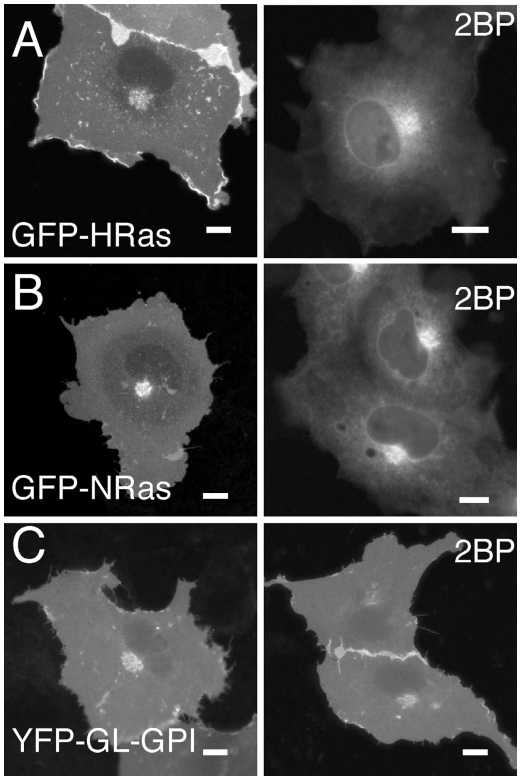

Figure 6. **2BP inhibits delivery of GFP-HRas and GFP-NRas, but not YFP-GL-GPI, to the cell surface.** COS-7 cells were treated with 2BP or vehicle overnight immediately after transfection with (A) GFP-HRas, (B) GFP-NRas, or (C) YFP-GL-GPI and imaged the following day. Bars, 10 μm.

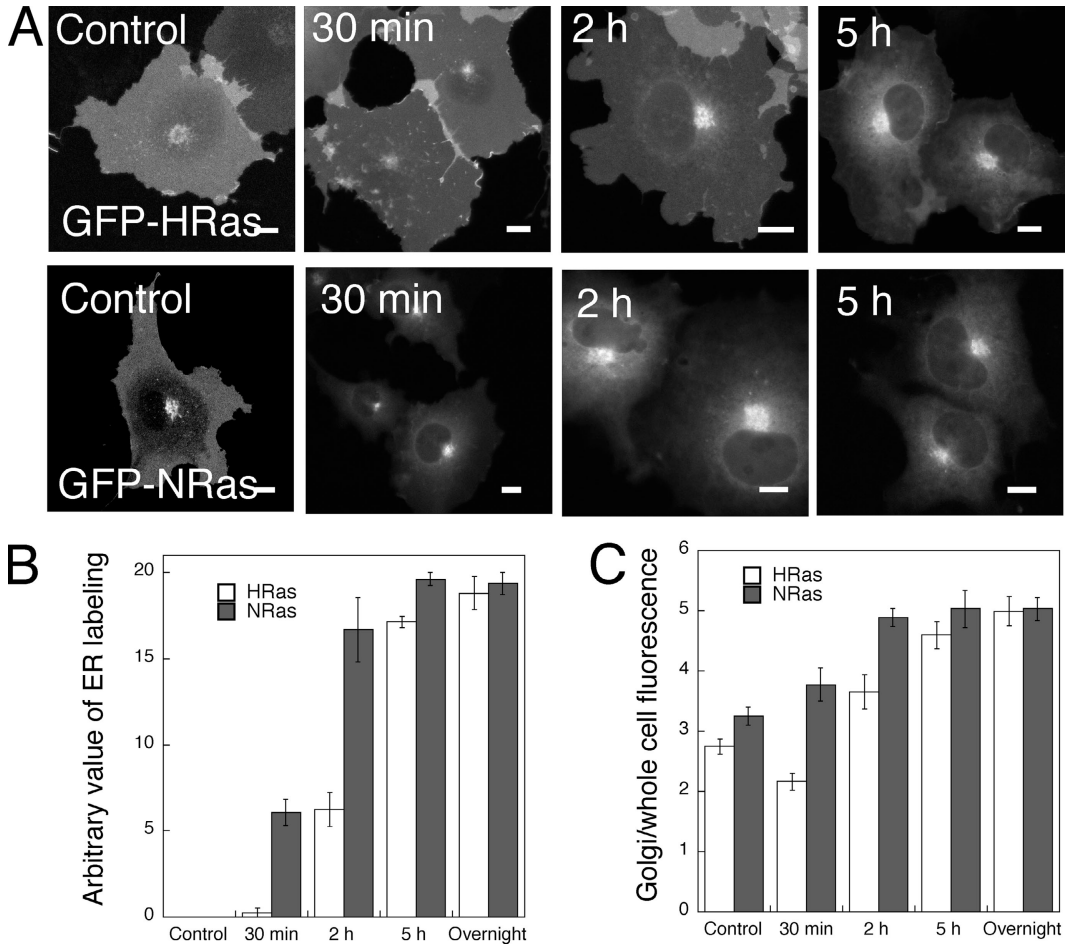

Figure 7. **Time course of redistribution of GFP-HRas and GFP-NRas in response to 2BP treatment.** (A) Cells were transfected with GFP-HRas or GFP-NRas, allowed to express the protein overnight, and then treated with 2BP for the indicated times before imaging. Bars, 10 μm. (B) Cells treated with 2BP were scored for ER labeling as described in Materials and methods. Data show the mean ± SE for four independent experiments. (C) Cells treated with 2BP were scored for the fraction of Ras localized to the Golgi complex as described in the Materials and methods. Data are the mean ± SE from three independent experiments.

trafficking, we examined the effect of an inhibitor of protein palmitoylation, 2-bromo-palmitate (2BP) (Webb et al., 2000). 2BP inhibits trafficking of newly synthesized HRas to the cell surface, causing it to accumulate on endomembranes (Michaelson et al., 2001, 2002) (Fig. 6, A and B). We confirmed that this is not due to a general defect in the secretory pathway because the cell surface expression of a GPI-anchored protein, YFP-GL-GPI, is unaffected by 2BP treatment (Fig. 6 C).

We reasoned that by blocking palmitoylation after Ras has been delivered to the cell surface, 2BP should cause the accumulation of depalmitoylated protein by preventing its repalmitoylation. To test this, we allowed GFP-HRas or GFP-NRas to be expressed overnight, treated with cycloheximide for 4 h to inhibit new protein synthesis, then treated the cells with 2BP for various times before imaging (Fig. 7 A). To quantitate the effect of 2BP on the subcellular distribution of Ras, we scored the fraction of cells exhibiting ER and/or nuclear envelope staining (Fig. 7 B). We also analyzed the ratio of fluorescence in the Golgi region versus the whole cell after 2BP treatment (Fig. 7 C). After 30 min of 2BP treatment, the fraction of NRas associated with the ER and Golgi complex was significantly increased; by 2 h, the distribution of the protein was similar to cells transfected in the presence of 2BP. GFP-HRas also redistributed to the ER and Golgi complex in response to 2BP treatment in a time-dependent manner, although the kinetics were slower than for GFP-NRas. Photobleaching experiments confirmed that the fraction of protein reversibly bound to the Golgi complex also increased over time after 2BP treatment (unpublished data). We conclude from these studies that depalmitoylation of Ras allows the protein to recycle from the cell surface to the ER and Golgi complex.

Discussion

In this study we examined the role of palmitoylation in the regulation of trafficking and subcellular localization of the two major palmitoylated Ras isoforms, HRas and NRas. Using time-lapse microscopy in combination with fluorescence photobleaching techniques, we show that GFP-tagged Ras palmitoylation mutants undergo rapid and reversible exchange between ER membranes, Golgi membranes, and the cytoplasm.

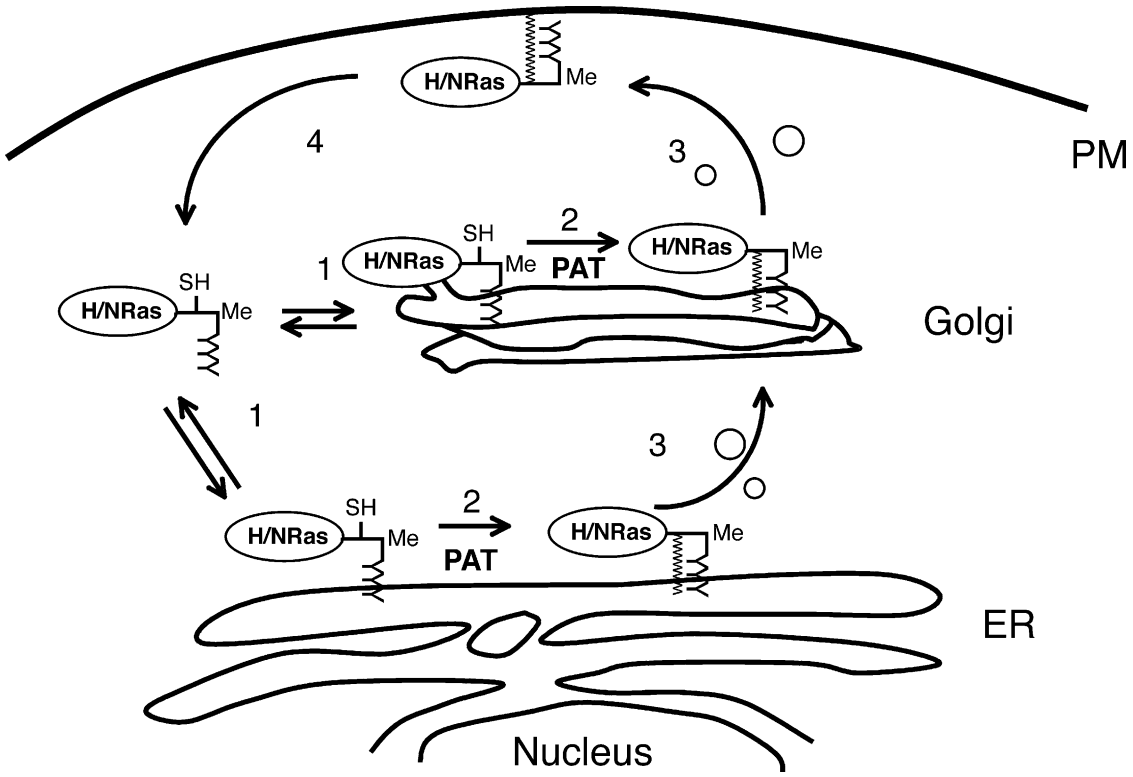

Figure 8. **Working model for how palmitoylation regulates HRas and NRas trafficking to and from the Golgi complex.** (1) Before palmitoylation, newly synthesized Ras can reversibly bind ER and Golgi membranes and traffic between them via a soluble cytosolic intermediate. (2) Palmitoylation via a putative palmitoyl acyl transferase (PAT) kinetically traps Ras onto membranes in the early secretory pathway, and (3) enables the protein to be packaged into vesicles bound for the cell surface. Once reaching the cell surface, palmitoylated HRas and NRas can undergo endocytosis (not depicted). (4) Turnover of palmitate generates a transiently depalmitoylated pool of protein that is returned to the Golgi complex and/or ER by nonvesicular transport, where it can again interact with PAT and reenter the secretory pathway.

We also find that wild-type GFP-HRas and GFP-NRas are recycled to the Golgi complex under steady-state conditions by a mechanism involving a cycle of depalmitoylation and repalmitoylation of the protein. Our data indicate that Ras shifts between vesicular and nonvesicular modes of transport depending on its palmitoylation state. These observations are summarized in a working model for how palmitoylation modulates HRas and NRas trafficking in Fig. 8. In this scenario, after farnesylation in the cytoplasm, newly synthesized Ras interacts with ER membranes, where enzymes involved in the processing of the Ras COOH terminus are localized (Dai et al., 1998; Schmidt et al., 1998; Zhao et al., 2002). Depending on the location of the putative Ras palmitoyltransferase, transport of Ras from the ER to Golgi complex occurs by either a nonvesicular or vesicular pathway. Once palmitoylated, HRas and NRas can be incorporated into Golgi-derived vesicles destined for the cell surface. Depalmitoylation of Ras by a putative acyl protein thioesterase or by nonenzymatic hydrolysis allows the protein to be released from the cell surface and return by a nonvesicular transport pathway to the Golgi complex and ER. Ras is then repalmitoylated in the early secretory pathway and reenters a vesicular transport pathway exiting the Golgi complex for the cell surface. This model is in excellent agreement with the results of a recent study examining the role of palmitoylation in the regulation of the subcellular localization and signaling of palmitoylated forms of Ras (Rocks et al., 2005).

Binding of nonpalmitoylated Ras to ER and Golgi membranes occurs independently of specific protein–protein interactions and is modulated by the nature of the prenyl group

Our in vivo measurements demonstrate that the CAAX motif is sufficient to mediate efficient but rapidly reversible binding of GFP to ER and Golgi membranes. These findings are in agreement with classic biochemical fractionation experiments showing that in the absence of a second signal, Ras exhibits reduced membrane binding affinity (Hancock et al., 1990). However, our data offer several new insights into the mechanisms underlying this reversible binding/partitioning. First, through quantitative comparison of fluorescence recovery kinetics, we find that Ras palmitoylation mutants and GFP-CVLS bind the Golgi complex with nearly equal affinity (Fig. 1). Similarly, in the ER, the behavior of GFP-CVLS and the palmitoylation mutants was indistinguishable via photobleaching or FCS criteria (Figs. 2 and 3). Thus, in the absence of palmitoylation, Ras membrane binding affinity is dominated by the COOH-terminal membrane anchor. Although these data suggest that this binding occurs independently of specific protein–protein interactions, the NH_2-terminal domain of Ras did appear to modestly enhance binding, as the halftimes of recovery for GFP-CVLS were slightly faster than the palmitoylation mutants. A more important contributor to binding is the hydrophobic nature of

the prenyl moiety, as GFP-CLLL, a substrate for geranylgeranylation, exhibited a twofold increase in binding compared with the farnesylated proteins examined in this study (Figs. 2 and 3). Interestingly, this difference is much smaller than that observed in in vitro studies, where geranylgeranylated peptides exhibit a 45-fold higher effective partition coefficient than farnesylated peptides (Silvius and l'Heureux, 1994). Other factors that could potentially modulate the membrane binding of CAAX-containing proteins to ER and Golgi membranes include postprenylation processing of the CAAX motif (Michaelson et al., 2005) and prenyl-binding proteins such as PRA1 (Figueroa et al., 2001). Binding to ER and Golgi membranes may also depend on the specific amino acid composition of the hypervariable domain, whether Ras is GTP or GDP bound, and the cholesterol content of the membrane, factors recently shown to regulate the strength of HRas binding to the plasma membrane (Rotblat et al., 2004).

Because nonpalmitoylated Ras has access to the cytosol, our findings raise the question of why it does not significantly bind the plasma membrane (Choy et al., 1999; Apolloni et al., 2000). One possibility is that the lipid composition of the ER and Golgi membranes is preferable for insertion of prenyl moieties. However, in vitro binding of prenylated peptides to liposomes show little dependence on membrane composition (Silvius and l'Heureux, 1994). Alternatively, membrane potential and/or electrostatic interactions, which presumably are responsible for the specific binding of KRas to the cell surface (Choy et al., 1999; Apolloni et al., 2000), may play an inhibitory role in preventing plasma membrane binding in the absence of a second plasma membrane binding signal. Finally, as discussed in the previous paragraph, putative prenyl binding proteins localized to the ER and Golgi complex could potentially act as sites for transient binding interactions.

The palmitoylation state of Ras determines whether the protein undergoes vesicular or nonvesicular transport

Our data suggest that Ras can shift between vesicular and nonvesicular transport by regulating its palmitoylation state in a manner consistent with the "kinetic trap" model of palmitoylation (Shahinian and Silvius, 1995). This model proposes that farnesylated (but nonpalmitoylated) peptides can efficiently but reversibly bind membranes until they are palmitoylated, trapping them on the membrane. Such kinetic trapping can readily explain why Ras palmitoylation mutants are rapidly and reversibly bound to membranes, whereas a substantial fraction of palmitoylated HRas and NRas is stably bound to the Golgi complex.

As an extension of this model, we propose that the intracellular sites at which Ras palmitoyl acyl transferase (PAT) enzymes reside define the entry points for Ras into vesicular transport pathways. For example, if PAT activity is present in the ER or intermediate compartment, newly synthesized Ras would enter into vesicles early in the secretary pathway. Conversely, if the PAT activity is localized exclusively at the plasma membrane, Ras could potentially traffic to the plasma membrane completely independently of vesicular transport. The latter possibility may explain why in adipocytes, delivery of HRas to the cell surface occurs in the presence of BFA or after a 20° block (Watson et al., 2003). This nonclassical cell surface transport pathway is an excellent candidate for regulation via a cycle of palmitoylation and depalmitoylation (Watson et al., 2003). A similar model could explain how peptides mimicking the NRas COOH terminus reach to the plasma membrane independent of the secretory pathway (Schroeder et al., 1997).

Our understanding of the role of palmitoylation in Ras trafficking will be greatly enhanced by the identification of the proteins responsible for this process. Although palmitoylation can occur by nonenzymatic means, there is evidence that in cells this is a regulated event (Dietrich and Ungermann, 2004; Smotrys and Linder, 2004). Although the enzymes responsible for palmitoyl transferase activity have long been sought (Kasinathan et al., 1990; Gutierrez and Magee, 1991; Berthiaume and Resh, 1995; Das et al., 1997), only recently have candidate Ras PATs been identified. Studies in yeast first identified an ER-localized protein complex, Erf2/Erf4, that stimulates palmitoylation of Ras2 in vitro (Lobo et al., 2002). These proteins contain a DHHC cysteine-rich domain that has been postulated to be a signature of proteins involved in palmitoylation (Smotrys and Linder, 2004). Very recently, several candidate mammalian Ras palmitoyltransferases have been identified (Ducker et al., 2004; Fukata et al., 2004; Huang et al., 2004). Given these recent breakthroughs, it should be possible to begin to directly dissect the role of these proteins in Ras localization and function in the near future.

It is important to note that the kinetic trapping model does not exclude other potential roles for palmitoylation in the regulation of Ras trafficking. For example, the yeast Ras homologue Ras2p is trafficked to the plasma membrane in the absence of a functional secretory pathway in a process requiring Erf2p, a putative ER-localized palmitoyltransferase, by an as-yet-unidentified mechanism (Dong et al., 2003). It is possible that palmitoylation-dependent interactions allow Ras to interact with chaperone proteins that traffic the protein by vesicle-independent pathways. Alternatively, palmitoylation-dependent targeting of Ras to raft-enriched or other types of membrane microdomains may be important for allowing it either to exit the Golgi complex (Magee and Marshall, 1999) or to be internalized from the cell surface by either clathrin-dependent or -independent endocytic pathways (Roy et al., 2002).

Regulation of the rate of depalmitoylation of NRas versus HRas

The potential for Ras to undergo multiple rounds of depalmitoylation and subsequent repalmitoylation were first suggested by studies of NRas, which indicated that the half-life of palmitate is shorter than the life span of the protein (Magee et al., 1987). One enzyme that has been demonstrated to remove palmitate from HRas in vitro is acyl-thioesterase 1 (Smotrys and Linder, 2004). However, much remains to be learned about how this event is regulated. Although it is tempting to speculate that the primary pool of Ras undergoing depalmitoylation is localized to the cell surface, it is unclear whether specific subcellular pools of Ras are preferred substrates for depalmitoylation.

Interestingly, we found that the rate of palmitate turnover differs for HRas and NRas. First, a larger fraction of wild-type NRas than HRas was reversibly bound to the Golgi complex (Fig. 4). This implies that a larger fraction of NRas than HRas is present in a depalmitoylated state under steady-state conditions. In addition, after 2BP treatment NRas redistributed to the ER and Golgi more rapidly than HRas (Fig. 6), suggesting that NRas undergoes a more rapid rate of depalmitoylation. These observations are consistent with reports that the half-life of palmitate on HRas, ranging from 90 min to 2.4 h (Lu and Hofmann, 1995; Baker et al., 2003), is relatively long compared with that of NRas (20 min) (Magee et al., 1987). Because HRas contains two palmitoylation sites compared with NRas's one, it is likely that the difference in overall half-lives reflects a higher probability that at least one palmitate will be present on HRas. Indeed, the half-life of palmitate on overexpressed HRas was previously shown to be reduced from ~90 min to 15 min upon mutation of one of the palmitoylation sites, with slower turnover correlating with stronger membrane binding (HRas Ser181) (Lu and Hofmann, 1995). This same study showed little evidence for specific recognition of palmitoylated proteins, thus suggesting that access to a depalmitoylating enzyme determined the palmitate turnover rate. Our finding that depalmitoylation plays a role in determining the subcellular distribution and trafficking of HRas and NRas highlights the need for further characterization of the regulation of these events.

Nature of the soluble pool of Ras

The presence of a soluble pool of Ras has been noted by several groups, with the fraction of soluble protein ranging from 10–20% to upwards of 40–50% (Magee et al., 1987; Hancock et al., 1990; Lu and Hofmann, 1995; Choy et al., 1999; Webb et al., 2000; Baker et al., 2003). Our data suggest that this soluble pool corresponds to transiently depalmitoylated Ras, in agreement with a previous study showing that soluble NRas is farnesylated but not palmitoylated (Magee et al., 1987). How Ras is solubilized in the presence of a farnesyl moiety is not yet known. Delivery of geranylgeranylated Rab proteins to membranes is mediated by Rab escort protein (REP) or a Rab GDP dissociation inhibitor (GDI) (for review see Seabra and Wasmeier, 2004). The prenylated Rab acceptor protein (PRA1) and phosphodiesterase-δ are two candidate Ras escort proteins (Figueroa et al., 2001; Hanzal-Bayer et al., 2002; Nancy et al., 2002). However, it should be noted that in vitro peptide binding experiments show that farnesylated proteins have an intrinsically weak affinity for membranes, and thus may not require a specialized mechanism to allow them to become solubilized (Silvius and l'Heureux, 1994). Yet another possibility, suggested by biochemical studies in progress, is that soluble farnesylated Ras exists as a dimer (unpublished data). Our FCS studies show that soluble Ras has a diffusional mobility similar to cytoplasmic GFP (Fig. 3, Table I). Given the weak dependence of diffusion on protein size, these data are consistent with the possibility that soluble Ras exists either as a monomer or in small complexes with itself or other proteins. More work will be required to distinguish between these possibilities.

Implications for Ras signaling

We envision several mechanisms by which the regulation of the palmitoylation state of Ras could control the intracellular location and time course of Ras signaling. First, the loss of palmitate on Ras may allow for the regulated release of the protein from the cell surface. Such an event could even be regulated by Ras activation itself, as the depalmitoylation of GTP-bound HRas is accelerated compared with the GDP-bound form (palmitate half-life of 10 min vs. 2.4 h, respectively) (Baker et al., 2003). Given that depalmitoylated Ras can still efficiently bind intracellular membranes, such an event may not have a large effect on the subcellular distribution of Ras as assessed by biochemical criteria. This could explain why 2BP treatment causes only a 7–20% increase in the soluble pool of HRas (Webb et al., 2000). After depalmitoylation, activated Ras could itself act as a diffusible signaling intermediate, allowing the protein to rapidly redistribute to other intracellular compartments. Evidence supporting this model was very recently reported (Peyker et al., 2005; Rocks et al., 2005). The reversible binding of depalmitoylated Ras may also explain the rapid (~2 min after stimulation) recruitment of GFP-RBD to ER membranes in cells overexpressing HRas palmitoylation mutants (Chiu et al., 2002). This also implies that reversible membrane binding of Ras is sufficient to enable efficient signaling. Finally, a cycle of depalmitoylation and repalmitoylation may regulate intracellular Ras signaling by maintaining a steady-state pool of Ras on the Golgi complex (Chiu et al., 2002; Bivona et al., 2003; Caloca et al., 2003; Mitin et al., 2004; Perez de Castro et al., 2004; Rocks et al., 2005). This may also contribute to the specific outcomes of HRas signaling in response to altered membrane-targeting signals (Booden et al., 1999, 2000; Coats et al., 1999). Disruption of Ras recycling to the Golgi complex may thus offer a potential mechanism to interfere with oncogenic Ras activity.

Materials and methods

DNA constructs, cell transfections, and fluorescent probes

COS-7 cells were maintained in DME supplemented with 10% fetal calf serum at 5% CO_2 and 37°C. Cells were transfected using FuGENE 6 (Roche Diagnostics) according manufacturer's protocol and imaged 1 and 2 d after transfection. cDNA for GFP-Ras chimeras (EGFP-CVLS, EGFP-CLLL, EGFP-HRas C181S, C184S, EGFP-NRas C181S, EGFP-HRas, and EGFP-NRas) and GFP-GPI were as previously described (Choy et al., 1999; Nichols et al., 2001). Note that no linkers were used in the construction of EGFP-CLLL and EGFP-CVSL. For simplicity, EGFP is referred to as GFP in the text. Control experiments confirmed that the CAAX motif of overexpressed GFP-Ras is quantitatively processed, and that in the absence of farnesylation the protein is not associated with any intracellular membranes (Fig. S1, available at http://www.jcb.org/cgi/content/full/jcb.200502063/DC1). CTXB (Sigma-Aldrich) was fluorescently labeled with Cy3 according to the manufacturer's instructions (GE Healthcare). Cells were labeled with 1 μg/ml Cy3-CTXB for 15 min on ice and washed several times before imaging or drug treatments.

Nocodazole and cycloheximide treatments

To disrupt microtubules, cells were preincubated for 5 min on ice in DME containing 10% fetal calf serum and 50 mM Hepes. The cells were then treated with 5 μg/ml nocodazole (Sigma-Aldrich) for 15 min on ice, warmed for 5 min to 37°C, and imaged in the continued presence of nocodazole at 37°C. Control experiments were performed using vehicle alone (DMSO). To inhibit new protein synthesis, cells were treated with 200 μg/ml cycloheximide (Sigma-Aldrich) in DME, 10% fetal calf serum, and 50 mM Hepes for 4 h at 37°C. The cells were then imaged at 37°C in the cycloheximide solution.

Fluorescence microscopy and photobleaching measurements

Cells were imaged with an inverted laser scanning confocal microscope (model 510; Carl Zeiss MicroImaging, Inc.) equipped with the Confocor2 for FCS (Carl Zeiss MicroImaging, Inc.). Where indicated, an Air Stream Stage Incubator (Nevtek) was used for imaging at 37°C. GFP was excited with an argon laser with excitation at 488 nm and emission was detected with a GFP long-pass (LP) 505 or 530 or band-pass (BP) 505–530 filter. A Plan-Neofluar 40×/1.3 oil immersion lens was used for imaging all samples. Cells were maintained in phenol-red free DME containing 10% fetal calf serum and 50 mM Hepes for live-cell imaging experiments.

Confocal FRAP measurements were performed using a previously described protocol (Kenworthy et al., 2004). In brief, a strip 4 μm wide was photobleached using high laser intensity and fluorescence recovery monitored at low intensity. Diffusion coefficients were calculated from whole-cell recoveries using a program that simulates diffusion (Siggia et al., 2000). Mf was calculated as described previously (Ellenberg et al., 1997). Statistical differences were evaluated using the *t* test.

In experiments measuring kinetics of Golgi refilling, an area containing the entire Golgi was bleached (Nichols et al., 2001). Halftimes of recovery were calculated as described in Feder et al. (1996), and the final percentage of recovered fluorescence was calculated as for Mf after correcting for the loss of fluorescence due to the photobleaching event. Control experiments on fixed cells confirmed that the loss of fluorescence was confined to the bleached region.

All quantitative image analysis was performed using unprocessed images. For presentation purposes, image contrast was adjusted using Adobe Photoshop.

Quantitation of Ras localization after 2BP treatment

Cells were treated with 25 μM 2BP (Sigma-Aldrich) or vehicle (DMSO) at 37°C, either immediately after transfection or 18 h after transfection for the indicated times (30 min, 2 h, or 5 h). After treatment, cells were imaged live with the confocal pinhole fully open for quantitation or set at 1–2 Airy units for presentation purposes. The subcellular distribution of Ras in ~20 cells/treatment was quantitated in two ways. (1) Localization of Ras in the ER/nuclear envelope versus plasma membrane. Cells were scored for the relative amounts of ER/nuclear envelope labeling ranging from ER labeling but no apparent plasma membrane stain (++++) to no apparent ER or nuclear envelope label (−−−−). These scores were converted to a numeric value as follows: ++++ (1 pt), +++/− (0.75 pt), ++/−− (0.5 pt), +/−−− (0.25 pt), or −−−− (0 pt). The total numeric score for all cells at a given time point was calculated for each experiment. (2) Fraction of Ras localized to the Golgi complex. Images were converted to tiff format, and the average fluorescence in the Golgi region versus in the entire cell was calculated using NIH Image. After background subtraction, the ratio of fluorescent material in the Golgi region versus the entire cell was calculated.

Fluorescence correlation spectroscopy

FCS measures time-dependent fluorescence fluctuations in a diffraction-limited (0.1 femtoliter) volume defined using confocal microscope optics with a sensitive avalanche photodiode detector. Intensity fluctuations corresponding to the movements of individual molecules in and out of the confocal volume are recorded over time. Fluorescence fluctuations reflect the average residence time of the fluorescent species in the confocal volume, which in turn are a function of its characteristic diffusional mobility. The diffusion of fluorescently tagged proteins through the sampling volume occurs with a characteristic τ_D. This is related to the diffusion coefficient *D* by $\tau_D = (\omega_0^2)/(4D)$, where ω_0 is the radius of the laser beam. Thus, a longer τ_D corresponds to a slower *D*. The intensity fluctuations are characterized by their average value $\langle I \rangle$ and their fluctuations $\delta I(t) = I(t) - \langle I \rangle$ and can be analyzed using an autocorrelation function $G(\tau)$. The normalized autocorrelation function is given by $G(\tau) = 1 + \langle \delta I(t) * \delta I(t + \tau) \rangle * \langle I \rangle^{-2}$, where I(t) is the time-dependent fluorescence intensity, τ is a short time interval after any arbitrary time t, and $\langle I \rangle$ is the mean value of fluorescence intensity.

FCS experiments were performed on a microscope (LSM 510; Carl Zeiss MicroImaging, Inc.) outfitted with ConfoCor2 (Carl Zeiss MicroImaging, Inc.), combining both FCS and confocal laser scanning capabilities. A C-Apochromat 40× 1.2 NA water objective was used in conjunction with a dichroic filter and 520-nm long-pass filter to focus and separate exciting and emitting radiation. GFP-tagged constructs were excited at 488 nm with a 40-mW argon laser. Aqueous rhodamine 6G solutions were used to calculate the confocal volume radius $\omega_0 = 1.44 \times 10^{-7}$ m, resulting in a confocal volume element of 0.1 fl.

Cells were imaged in LSM mode and, after selection of an appropriate cell, whole cells were repeatedly bleached to reduce the fluorescence to allow for FCS measurements. A line scan in the axial direction was performed to set the volume element at an appropriate position in the cell. FCS measurements were made for 10 s each and repeated 10 times per cell. The autocorrelation curves were fit using software provided by the manufacturer. The autocorrelation function $G(\tau)$ for a two-component model is described by the following equation: $G(\tau) = 1 + (1/N)\,[(1 - Y)(1 + \tau/\tau_{D1})^{-1}(1 + \tau/S^2\,\tau_{D1})^{-1/2} + Y(1 + \tau/\tau_{D2})^{-1}(1 + \tau/S^2\,\tau_{D2})^{-1/2}]$.

Here, N is the number of fluorescent particles in the confocal volume; S is the structure parameter (defined by the dimensions of the confocal volume); τ_{D1} and τ_{D2} are the average residence times of the first and second component, respectively; and Y and $1 - Y$ are the fraction of particles in the confocal volume with diffusion time τ_{D2} and τ_{D1}, respectively. Data were fit assuming a constant structure parameter of 5.0. Diffusion coefficients were calculated from the fitted values of τ_D and the known confocal radius ω_0 as described above. Data were obtained from 10–20 cells from two independent experiments.

Online supplemental material

The online supplemental material describes control experiments performed to test whether overexpressed GFP-Ras fusion proteins are quantitatively farnesylated, and is available at http://www.jcb.org/cgi/content/full/jcb.200502063/DC1.

We thank Jan Buss and Ben Nichols for helpful discussions.

A. Kenworthy was supported by a fellowship from the National Research Council and a New Faculty Development Award from the Department of Molecular Physiology and Biophysics, Vanderbilt University School of Medicine.

Submitted: 10 February 2005
Accepted: 15 June 2005

References

Apolloni, A., I.A. Prior, M. Lindsay, R.G. Parton, and J.F. Hancock. 2000. H-ras but not K-ras traffics to the plasma membrane through the exocytic pathway. *Mol. Cell. Biol.* 20:2475–2487.

Baker, T.L., M.A. Booden, and J.E. Buss. 2000. S-nitrosocysteine increases palmitate turnover on Ha-Ras in NIH 3T3 cells. *J. Biol. Chem.* 275: 22037–22047.

Baker, T.L., H. Zheng, J. Walker, J.L. Coloff, and J.E. Buss. 2003. Distinct rates of palmitate turnover on membrane-bound cellular and oncogenic H-ras. *J. Biol. Chem.* 278:19292–19300.

Berthiaume, L., and M.D. Resh. 1995. Biochemical characterization of a palmitoyl acyltransferase activity that palmitoylates myristoylated proteins. *J. Biol. Chem.* 270:22399–22405.

Bivona, T.G., and M.R. Philips. 2003. Ras pathway signaling on endomembranes. *Curr. Opin. Cell Biol.* 15:136–142.

Bivona, T.G., I. Perez De Castro, I.M. Ahearn, T.M. Grana, V.K. Chiu, P.J. Lockyer, P.J. Cullen, A. Pellicer, A.D. Cox, and M.R. Philips. 2003. Phospholipase Cγ activates Ras on the Golgi apparatus by means of RasGRP1. *Nature.* 424:694–698.

Booden, M.A., T.L. Baker, P.A. Solski, C.J. Der, S.G. Punke, and J.E. Buss. 1999. A non-farnesylated Ha-Ras protein can be palmitoylated and trigger potent differentiation and transformation. *J. Biol. Chem.* 274:1423–1431.

Booden, M.A., D.S. Sakaguchi, and J.E. Buss. 2000. Mutation of Ha-Ras C terminus changes effector pathway utilization. *J. Biol. Chem.* 275:23559–23568.

Caloca, M.J., J.L. Zugaza, and X.R. Bustelo. 2003. Exchange factors of the RasGRP family mediate Ras activation in the Golgi. *J. Biol. Chem.* 278:33465–33473.

Chiu, V.K., T. Bivona, A. Hach, J.B. Sajous, J. Stilleti, H. Wiener, R.L. Johnson, A.D. Cox, and M.R. Philips. 2002. Ras signalling on the endoplasmic reticulum and the Golgi. *Nat. Cell Biol.* 4:343–350.

Choudhury, A., M. Dominguez, V. Puri, D.K. Sharma, K. Narita, C.L. Wheatley, D.L. Marks, and R.E. Pagano. 2002. Rab proteins mediate Golgi transport of caveola-internalized glycosphingolipids and correct lipid trafficking in Niemann-Pick C cells. *J. Clin. Invest.* 109:1541–1550.

Choy, E., V.K. Chiu, J. Silletti, M. Feoktistov, T. Morimoto, D. Michaelson, I.E. Ivanov, and M.R. Philips. 1999. Endomembrane trafficking of Ras: the CAAX motif targets proteins to the ER and Golgi. *Cell.* 98:69–80.

Clarke, S. 1992. Protein isoprenylation and methylation at carboxyl-terminal cysteine residues. *Annu. Rev. Biochem.* 61:355–386.

Coats, S.G., M.A. Booden, and J.E. Buss. 1999. Transient palmitoylation supports H-Ras membrane binding but only partial biological activity. *Biochemistry.* 38:12926–12934.

Dai, Q., E. Choy, V. Chiu, J. Romano, S.R. Slivka, S.A. Steitz, S. Michaelis, and

M.R. Philips. 1998. Mammalian prenylcysteine carboxyl methyltransferase is in the endoplasmic reticulum. *J. Biol. Chem.* 273:15030–15034.

Das, A.K., B. Dasgupta, R. Bhattacharya, and J. Basu. 1997. Purification and biochemical characterization of a protein-palmitoyl acyltransferase from human erythrocytes. *J. Biol. Chem.* 272:11021–11025.

Dietrich, L.E., and C. Ungermann. 2004. On the mechanism of protein palmitoylation. *EMBO Rep.* 5:1053–1057.

Dittrich, P., F. Malvezzi-Campeggi, M. Jahnz, and P. Schwille. 2001. Accessing molecular dynamics in cells by fluorescence correlation spectroscopy. *Biol. Chem.* 382:491–494.

Dong, X., D.A. Mitchell, S. Lobo, L. Zhao, D.J. Bartels, and R.J. Deschenes. 2003. Palmitoylation and plasma membrane localization of Ras2p by a nonclassical trafficking pathway in *Saccharomyces cerevisiae*. *Mol. Cell. Biol.* 23:6574–6584.

Downward, J. 2003. Targeting RAS signalling pathways in cancer therapy. *Nat. Rev. Cancer.* 3:11–22.

Ducker, C.E., E.M. Stettler, K.J. French, J.J. Upson, and C.D. Smith. 2004. Huntingtin interacting protein 14 is an oncogenic human protein: palmitoyl acyltransferase. *Oncogene.* 23:9230–9237.

Ellenberg, J., E.D. Siggia, J.E. Moreira, C.L. Smith, J.F. Presley, H.J. Worman, and J. Lippincott-Schwartz. 1997. Nuclear membrane dynamics and reassembly in living cells: targeting of an inner nuclear membrane protein in interphase and mitosis. *J. Cell Biol.* 138:1193–1206.

Feder, T.J., I. Brust-Mascher, J.P. Slattery, B. Baird, and W.W. Webb. 1996. Constrained diffusion or immobile fraction on cell surfaces: a new interpretation. *Biophys. J.* 70:2767–2773.

Figueroa, C., J. Taylor, and A.B. Vojtek. 2001. Prenylated Rab acceptor protein is a receptor for prenylated small GTPases. *J. Biol. Chem.* 276:28219–28225.

Fukata, M., Y. Fukata, H. Adesnik, R.A. Nicoll, and D.S. Bredt. 2004. Identification of PSD-95 palmitoylating enzymes. *Neuron.* 44:987–996.

Gutierrez, L., and A.I. Magee. 1991. Characterization of an acyltransferase acting on p21N-ras protein in a cell-free system. *Biochim. Biophys. Acta.* 1078:147–154.

Hancock, J.F. 2003. Ras proteins: different signals from different locations. *Nat. Rev. Mol. Cell Biol.* 4:373–384.

Hancock, J.F., A.I. Magee, J.E. Childs, and C.J. Marshall. 1989. All ras proteins are polyisoprenylated but only some are palmitoylated. *Cell.* 57:1167–1177.

Hancock, J.F., H. Paterson, and C.J. Marshall. 1990. A polybasic domain or palmitoylation is required in addition to the CAAX motif to localize p21ras to the plasma membrane. *Cell.* 63:133–139.

Hancock, J.F., K. Cadwallader, and C.J. Marshall. 1991a. Methylation and proteolysis are essential for efficient membrane binding of prenylated p21K-ras(B). *EMBO J.* 10:641–646.

Hancock, J.F., K. Cadwallader, H. Paterson, and C.J. Marshall. 1991b. A CAAX or a CAAL motif and a second signal are sufficient for plasma membrane targeting of ras proteins. *EMBO J.* 10:4033–4039.

Hanzal-Bayer, M., L. Renault, P. Roversi, A. Wittinghofer, and R.C. Hillig. 2002. The complex of Arl2-GTP and PDEδ: from structure to function. *EMBO J.* 21:2095–2106.

Hirschberg, K., C.M. Miller, J. Ellenberg, J.F. Presley, E.D. Siggia, R.D. Phair, and J. Lippincott-Schwartz. 1998. Kinetic analysis of secretory protein traffic and characterization of Golgi to plasma membrane transport intermediates in living cells. *J. Cell Biol.* 143:1485–1503.

Huang, K., A. Yanai, R. Kang, P. Arstikaitis, R.R. Singaraja, M. Metzler, A. Mullard, B. Haigh, C. Gauthier-Campbell, C.A. Gutekunst, et al. 2004. Huntingtin-interacting protein HIP14 is a palmitoyl transferase involved in palmitoylation and trafficking of multiple neuronal proteins. *Neuron.* 44:977–986.

Kasinathan, C., E. Grzelinska, K. Okazaki, B.L. Slomiany, and A. Slomiany. 1990. Purification of protein fatty acyltransferase and determination of its distribution and topology. *J. Biol. Chem.* 265:5139–5144.

Kato, K., A.D. Cox, M.M. Hisaka, S.M. Graham, J.E. Buss, and C.J. Der. 1992. Isoprenoid addition to Ras protein is the critical modification for its membrane association and transforming activity. *Proc. Natl. Acad. Sci. USA.* 89:6403–6407.

Katz, M.E., and F. McCormick. 1997. Signal transduction from multiple Ras effectors. *Curr. Opin. Genet. Dev.* 7:75–79.

Kenworthy, A.K., B.J. Nichols, C.L. Remmert, G.M. Hendrix, M. Kumar, J. Zimmerberg, and J. Lippincott-Schwartz. 2004. Dynamics of putative raft-associated proteins at the cell surface. *J. Cell Biol.* 165:735–746.

Linder, M.E., and R.J. Deschenes. 2003. New insights into the mechanisms of protein palmitoylation. *Biochemistry.* 42:4311–4320.

Linder, M.E., and R.J. Deschenes. 2004. Model organisms lead the way to protein palmitoyltransferases. *J. Cell Sci.* 117:521–526.

Lobo, S., W.K. Greentree, M.E. Linder, and R.J. Deschenes. 2002. Identification of a Ras palmitoyltransferase in *Saccharomyces cerevisiae*. *J. Biol. Chem.* 277:41268–41273.

Lu, J.Y., and S.L. Hofmann. 1995. Depalmitoylation of CAAX motif proteins. Protein structural determinants of palmitate turnover rate. *J. Biol. Chem.* 270:7251–7256.

Magee, A.I., I. Gutierrez, C.J. Marshall, and A. Hall. 1987. Dynamic fatty acylation of p21N-ras. *EMBO J.* 6:3353–3357.

Magee, T., and C. Marshall. 1999. New insights into the interaction of Ras with the plasma membrane. *Cell.* 98:9–12.

Michaelson, D., J. Silletti, G. Murphy, P. D'Eustachio, M. Rush, and M.R. Philips. 2001. Differential localization of Rho GTPases in live cells: regulation by hypervariable regions and RhoGDI binding. *J. Cell Biol.* 152:111–126.

Michaelson, D., I. Ahearn, M. Bergo, S. Young, and M. Philips. 2002. Membrane trafficking of heterotrimeric G proteins via the endoplasmic reticulum and Golgi. *Mol. Biol. Cell.* 13:3294–3302.

Michaelson, D., W. Ali, V.K. Chiu, M. Bergo, J. Silletti, L. Wright, S.G. Young, and M. Philips. 2005. Postprenylation CAAX processing is required for proper localization of Ras but not Rho GTPases. *Mol Biol Cell.* 16:1606–1616.

Mitin, N.Y., M.B. Ramocki, A.J. Zullo, C.J. Der, S.F. Konieczny, and E.J. Taparowsky. 2004. Identification and characterization of rain, a novel Ras-interacting protein with a unique subcellular localization. *J. Biol. Chem.* 279:22353–22361.

Nancy, V., I. Callebaut, A. El Marjou, and J. de Gunzburg. 2002. The δ subunit of retinal rod cGMP phosphodiesterase regulates the membrane association of Ras and Rap GTPases. *J. Biol. Chem.* 277:15076–15084.

Nehls, S., E.L. Snapp, N.B. Cole, K.J. Zaal, A.K. Kenworthy, T.H. Roberts, J. Ellenberg, J.F. Presley, E. Siggia, and J. Lippincott-Schwartz. 2000. Dynamics and retention of misfolded proteins in native ER membranes. *Nat. Cell Biol.* 2:288–295.

Nichols, B.J., A.K. Kenworthy, R.S. Polishchuk, R. Lodge, T.H. Roberts, K. Hirschberg, R.D. Phair, and J. Lippincott-Schwartz. 2001. Rapid cycling of lipid raft markers between the cell surface and Golgi complex. *J. Cell Biol.* 153:529–541.

Niv, H., O. Gutman, Y. Kloog, and Y.I. Henis. 2002. Activated K-Ras and H-Ras display different interactions with saturable nonraft sites at the surface of live cells. *J. Cell Biol.* 157:865–872.

Olson, M.F., and R. Marais. 2000. Ras protein signalling. *Semin. Immunol.* 12:63–73.

Parton, R.G., and J.F. Hancock. 2004. Lipid rafts and plasma membrane microorganization: insights from Ras. *Trends Cell Biol.* 14:141–147.

Perez de Castro, I., T.G. Bivona, M.R. Philips, and A. Pellicer. 2004. Ras activation in Jurkat T cells following low-grade stimulation of the T-cell receptor is specific to N-Ras and occurs only on the Golgi apparatus. *Mol. Cell. Biol.* 24:3485–3496.

Peyker, A., O. Rocks, and P.I. Bastiaens. 2005. Imaging activation of two Ras isoforms simultaneously in a single cell. *ChemBioChem.* 6:78–85.

Rocks, O., A. Peyker, M. Kahms, P.J. Verveer, C. Koerner, M. Lumbierres, J. Kuhlmann, H. Waldmann, A. Wittinghofer, and P.I. Bastiaens. 2005. An acylation cycle regulates localization and activity of palmitoylated Ras isoforms. *Science.* 307:1746–1752.

Rotblat, B., I.A. Prior, C. Muncke, R.G. Parton, Y. Kloog, Y.I. Henis, and J.F. Hancock. 2004. Three separable domains regulate GTP-dependent association of H-ras with the plasma membrane. *Mol. Cell. Biol.* 24:6799–6810.

Roy, S., B. Wyse, and J.F. Hancock. 2002. H-Ras signaling and K-Ras signaling are differentially dependent on endocytosis. *Mol. Cell. Biol.* 22:5128–5140.

Schmidt, W.K., A. Tam, K. Fujimura-Kamada, and S. Michaelis. 1998. Endoplasmic reticulum membrane localization of Rce1p and Ste24p, yeast proteases involved in carboxyl-terminal CAAX protein processing and amino-terminal a-factor cleavage. *Proc. Natl. Acad. Sci. USA.* 95:11175–11180.

Schroeder, H., R. Leventis, S. Rex, M. Schelhaas, E. Nagele, H. Waldmann, and J.R. Silvius. 1997. S-acylation and plasma membrane targeting of the farnesylated carboxyl-terminal peptide of N-ras in mammalian fibroblasts. *Biochemistry.* 36:13102–13109.

Seabra, M.C., and C. Wasmeier. 2004. Controlling the location and activation of Rab GTPases. *Curr. Opin. Cell Biol.* 16:451–457.

Shahinian, S., and J.R. Silvius. 1995. Doubly-lipid-modified protein sequence motifs exhibit long-lived anchorage to lipid bilayer membranes. *Biochemistry.* 34:3813–3822.

Shields, J.M., K. Pruitt, A. McFall, A. Shaub, and C.J. Der. 2000. Understanding Ras: 'it ain't over 'til it's over'. *Trends Cell Biol.* 10:147–154.

Siggia, E.D., J. Lippincott-Schwartz, and S. Bekiranov. 2000. Diffusion in inhomogeneous media: theory and simulations applied to whole cell photobleach recovery. *Biophys. J.* 79:1761–1770.

Silvius, J.R. 2002. Mechanisms of Ras protein targeting in mammalian cells. *J. Membr. Biol.* 190:83–92.

Silvius, J.R., and F. l'Heureux. 1994. Fluorimetric evaluation of the affinities of isoprenylated peptides for lipid bilayers. *Biochemistry.* 33:3014–3022.

Smotrys, J.E., and M.E. Linder. 2004. Palmitoylation of intracellular signaling proteins: regulation and function. *Annu. Rev. Biochem.* 73:559–587.

Ward, T.H., R.S. Polishchuk, S. Caplan, K. Hirschberg, and J. Lippincott-Schwartz. 2001. Maintenance of Golgi structure and function depends on the integrity of ER export. *J. Cell Biol.* 155:557–570.

Watson, R.T., M. Furukawa, S.H. Chiang, D. Boeglin, M. Kanzaki, A.R. Saltiel, and J.E. Pessin. 2003. The exocytotic trafficking of TC10 occurs through both classical and nonclassical secretory transport pathways in 3T3L1 adipocytes. *Mol. Cell. Biol.* 23:961–974.

Webb, Y., L. Hermida-Matsumoto, and M.D. Resh. 2000. Inhibition of protein palmitoylation, raft localization, and T cell signaling by 2-bromopalmitate and polyunsaturated fatty acids. *J. Biol. Chem.* 275:261–270.

Willumsen, B.M., A. Christensen, N.L. Hubbert, A.G. Papageorge, and D.R. Lowy. 1984. The p21 *ras* C-terminus is required for transformation and membrane association. *Nature.* 310:583–586.

Zaal, K.J.M., C.L. Smith, R.S. Polishchuk, N. Altan, N.B. Cole, J. Ellenberg, K. Hirschberg, J.F. Presley, T.H. Roberts, E. Siggia, et al. 1999. Golgi membranes are absorbed into and reemerge from the ER during mitosis. *Cell.* 99:589–601.

Zhao, L., S. Lobo, X. Dong, A.D. Ault, and R.J. Deschenes. 2002. Erf4p and Erf2p form an endoplasmic reticulum-associated complex involved in the plasma membrane localization of yeast Ras proteins. *J. Biol. Chem.* 277:49352–49359.